The ventral striatum in goal-directed behavior and sleep: intrinsic network dynamics, motivational information and relation with the hippocampus

Lansink, C.S.

Publication date
2008

CHAPTER 3

Fast-spiking interneurons of the rat ventral striatum: temporal coordination of activity with principal cells and responsiveness to reward

Carien S. Lansink, Pieter M. Goltstein, Jan V. Lankelma and Cyriel M.A. Pennartz

Submitted

Abstract

Whereas previous *in vitro* studies revealed inhibitory synaptic connections of fast-spiking interneurons to principal cells in the striatum, uncertainty remains about the nature of behavioral events that correlate with changes in interneuron activity and about the temporal coordination of interneuron firing with spiking of principal cells under natural conditions. Using *in vivo* tetrode recordings from ventral striatum in freely moving rats, fast-spiking neurons were distinguished from putative medium-sized spiny neurons on the basis of their spike waveforms and other firing characteristics. Cross-correlograms of fast-spiking and putative medium-sized spiny neuron firing patterns revealed a variety of temporal relationships, including a subset showing a transient decrement in medium-sized spiny neuron spiking around the moment the fast-spiking unit fired. Notably, the onset of these decrements was mostly in advance of fast-spiking unit firing. Coordinated activity was also found amongst pairs of fast-spiking units, often marked by broadly enhanced concurrent firing. When firing behavior of fast-spiking neurons was studied in relation to behavioral events in a reward-searching task, they were generally found to show a decrement in firing rate specifically when the rat received a reward, whereas the large majority of putative medium-sized spiny neurons, when responsive to this event, increased their firing rate.

In conclusion, our data indicate that the decrements in firing rate of medium-sized spiny neurons concurrent with fast-spiking activity are most parsimoniously explained by a partially synchronized network of interneurons that collectively inhibit firing of principal cells. Furthermore, firing patterns of ventral striatal fast-spiking interneurons display distinct post-reward decrements in firing rate.

Introduction

The ventromedial sector of the striatum (VS), which contains the nucleus accumbens as its main component, plays a role in invigorating and adjusting emotional and goal-directed behaviors (Mogenson et al., 1980; Pennartz et al., 1994; Berridge and Robinson, 1998; Cardinal et al., 2002; Kelley, 2004; Voorn et al., 2004; Salamone et al., 2005). Clinically, the VS has been implied in a considerable number of disorders, ranging from drug addiction to obsessive-compulsive disorder, depression and schizophrenia (Laruelle et al., 2003; Sturm et al., 2003; Everitt and Robbins, 2005; Kalivas and Volkow, 2005; Nestler and Carlezon, 2006). Whereas the principal cells of the striatum, i.e. medium-sized spiny neurons (MSNs), comprise ~90-95% of all neurons in this structure and have been extensively studied, much less is known about the functioning of an important class of its interneurons, viz. those generating 'fast' (i.e. short-lasting) action

potentials (fast-spiking interneurons, FSIs). Most of our knowledge on striatal FSIs has been gained in intracellular recordings from striatal slices maintained *in vitro*, and in immunocytochemical studies. FSIs express the calcium-buffering protein parvalbumin, and have aspiny dendrites and axon collaterals reaching nearby and more distant subregions of the striatum (Cowan et al., 1990; Kita et al., 1990; Kawaguchi, 1993; Kawaguchi et al., 1995). *In vitro*, striatal FSIs are capable of inhibiting firing of MSNs when these are depolarized by intracellular current injections (Koos and Tepper, 1999; Koos et al., 2004). Dual-cell recordings in acutely prepared slices showed that inhibition of MSNs by FSIs is mediated by $GABA_A$ receptors, both in dorsal (Koos and Tepper, 1999; Koos et al., 2004) and ventral striatum (Taverna et al., 2007). Functionally, FSIs in the VS are thought to provide feed-forward inhibition of MSNs, thereby shunting glutamatergic limbic and prefrontal inputs, and simultaneously exerting an inhibitory control over induction of long-term potentiation or other persistent synaptic changes in glutamatergic inputs onto MSNs (Pennartz and Kitai, 1991; Pennartz et al., 1993; 1994; Thomas et al., 2000).

Despite these *in vitro* results, the functional behavior of striatal FSIs under naturalistic behavioral conditions remains largely unknown. One may hypothesize that these neurons subserve a general role in sustaining a characteristic dynamic EEG state (e.g. oscillatory) within the striatum or, for instance, a homeostatic role in preventing a hyperexcitable state in case of massive glutamatergic input (cf. Mallet et al., 2005). An alternative but not mutually exclusive hypothesis holds that FSIs code task-related information in the sense that their spike timing or mean firing rate shows changes that correlate with discrete behavioral task phases or external events. We investigated the validity of the latter alternative by making tetrode recordings from the VS of awake and resting rats and examining FSI firing patterns in relation to the rat´s behavior on a reward-searching task set on a running track.

Another major question arising from previous *in vitro* studies is whether FSI activity is functionally effective in inhibiting firing of MSNs in non-anesthetized animals, when spikes are not artifically induced by somatic current injections. Thus, we studied the temporal coordination between FSIs and putative MSNs firing by way of cross-correlograms based on firing patterns recorded during resting conditions. Cross-correlograms provide useful information about the functional connectivity of neurons *in vivo* (Aertsen et al., 1989) and, when revealing short-latency interactions, can be indicative of monosynaptic interactions (e.g. Csicsvari et al., 2003). Besides examining putative inhibition from FSIs onto MSNs, we also asked whether MSNs may show a 'rebound excitation' following

FSI spiking, as has been found for interactions between hippocampal interneurons and pyramidal cells (Buhl et al., 1995; Cobb et al., 1995). Results for putative FSI-MSN pairs in VS were subsequently compared with temporal relationships found for FSI-FSI or MSN-MSN pairs. When present, coordinated activity amongst FSIs themselves may be important in generating rhythmic mass activity in the striatum *in vivo*, given that FSIs in VS have been reported to be entrained to striatal theta oscillations (Berke et al., 2004).

Results

Two main types of ventral striatal units

Spike waveforms and firing properties of a total of 256 VS units were recorded during behaviorally active or resting-sleeping conditions. Of these units, 148 were sufficiently active during rest periods to be eligible for the cross-correlation analysis. Two main classes of units could be distinguished on the basis of waveform properties (see Experimental Procedures), mean firing rates and firing pattern during a behavioral task. First, analysis of waveform properties indicated that the spike decay phase was well suited to segregate fast-spiking (FS) units from other units with broader spikes and slower decay of the spike valley (Fig. 3.1; Table 3.1). When two decay parameters were plotted against each other (i.e., the half-decay time vs. initial slope of valley decay; Fig. 3.1C) and a clustering algorithm was applied to discard units whose membership of a cell cluster was below an 80% certainty threshold, one cluster of 20 FS units and one of 114 other units were found. As an additional verification of spiking differences between the two clusters, their mean firing rates were found to differ dramatically (FS units during rest: 12.0 $\pm$ 2.0 Hz; others: 0.55 $\pm$ 0.07; $P < 1.10^{-6}$, Mann-Whitney U-test). These and other numerical values throughout the text represent means $\pm$ SEM unless otherwise noted. Considering that medium-sized spiny neurons (MSNs) make up the vast majority of striatal neurons (~90-95%; Kemp and Powell, 1971; Groves, 1983; Chang and Kitai, 1985; Gerfen and Wilson, 1996) these other units are likely to be of this type, but nevertheless it cannot be excluded that this group might contain a few tonically active (presumably cholinergic) neurons (Kimura et al., 1984; Apicella et al., 1991a; Bennett and Wilson, 1999). The short-lasting spikes with rapid decay found for FS units are well in agreement with the patch-clamp data from immunocytochemically identified, parvalbumin-positive GABAergic interneurons (Kawaguchi, 1993; Kawaguchi et al., 1995; Taverna et al., 2007). Similarly, morphologically identified MSNs have broader spikes and, in vivo, exhibit phasic firing patterns at low mean rate (Wilson and Groves, 1981; Taverna et al., 2004; Mahon et al., 2006). Nevertheless, we wish to emphasize that the identifications that can be made from extracellular spike recordings are less certain than in vitro; therefore we will designate a putative MSN as “pMSN” and not as “MSN”.

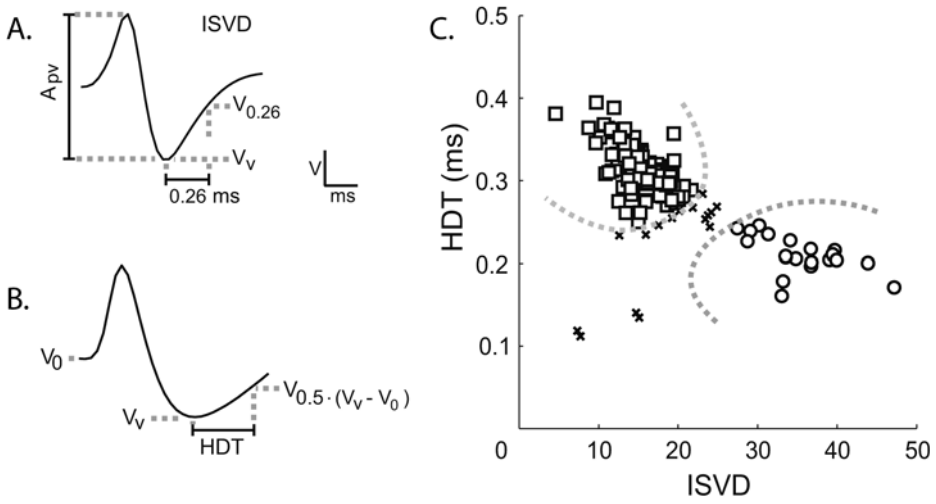

Figure 3.1

Spike waveforms and classification of fast-spiking (FS) units and putative medium-sized spiny neurons (pMSNs). A: Spike waveform of a representative FS unit. B: Idem, but now for a representative pMSN. Note the broader spike and slower decay of the spike valley towards baseline. Furthermore the plots show how the parameters Initial Slope of Valley Decay (ISVD; A) and Half-Decay Time (HDT; B) were computed; V_v is the most negative value (valley point) of the spike waveform in the plot, $V_{0.26}$ the voltage at 0.26 ms after V_v, A_{pv} the peak-to-valley amplitude and V_0 the baseline voltage (note, however, that negative polarity of voltage is plotted upward). C: Plot of HDT values against ISVD for 148 units eligible for the cross-correlation analysis. The graph shows two distinct groups of data points, corresponding to FS units (open circles; N=20) and pMSNs (open squares; N=114). Some units (crosses, N= 14) did not exceed the 80% certainty threshold for belonging to one of the two clusters (boundaries indicated by dashed lines) in a fuzzy clustering algorithm and were therefore not classified as FS unit or pMSN.

Temporal relationships between firing patterns of fast-spiking units and putative medium-sized spiny neurons

Previous *in vitro* studies on dorsal and ventral striatum suggest marked inhibitory interactions between fast-spiking interneurons and MSNs (Koos and Tepper, 1999; Taverna et al., 2007). These interactions are predicted to be dominated by FSI-to-MSN inhibition, although additional effects, such as rebound excitation after FS-mediated inhibition of MSNs, may also be found (cf. Plenz, 2003). In our current study, functional interactions between FS units and pMSNs were studied by way of cross-correlograms obtained from neurons recorded in both experiment 1 and 2 (with a total of 20 FS units and 114 pMSNs). These diagrams were based on rest-sleep episodes rather than active behavior to avoid

spurious correlations induced by coinciding neural responses to behavioral events (cf. Brody, 1999). A prerequisite for making accurate cross-correlograms is the availability of sufficient spike counts. This prerequisite was fulfilled for many FS-pMSN pairs, particularly due to the high mean firing rate of FS units. Indeed, the mean firing rate during resting and sleeping was over twenty times higher for FS than for pMSN units (Table 3.1).

Table 3.1: Waveform characteristics and firing rates for fast spiking (FS) units and putative medium sized spiny neurons (pMSNs)

	FS units	*n*	pMSNs	*n*
Subset experiment 1 & 2 for cross-correlation analysis		20		114
ISVD	35.0 ± 1.1		15.0 ± 0.3	
HDT (ms)	0.20 ± 0.00		0.31 ± 0.00	
Firing rate 'rest' (Hz)	12.0 ± 2.0		0.55 ± 0.07	
Experiment 1		10		190
Firing rate 'active bahavior' (Hz)	21.5 ± 4.0		0.23 ± 0.05	
Firing rate 'rest' (Hz)	9.7± 2.5		0.17 ± 0.05	

Waveform measures and firing rates for different groups of FS units and pMSNs. 'Experiment 1' contained a total of 10 FS units as well as 190 simultaneously recorded pMSNs. A substantial part of these pMSNs fired at very low rates during the rest episodes and therefore did not contribute to the cross-correlogram analysis. The firing rates during active behavior and rest were significantly higher for FS units than for pMSNs (Mann-Whitney-U test, $p < 1.10^{-6}$). Both FS units and pMSNs showed significantly higher rates during active behavior than during rest (Wilcoxon matched pairs signed rank test, FS units: $p < 0.005$, pMSNs: $p < 1.10^{-4}$). 'Subsets from Exp 1 and 2 for cross-correlation' comprise those neurons that were sufficiently active during the rest phase and were classified as FS unit or pMSN. The average firing rate during the rest period was significantly different between the FS units and pMSNs in these subsets (Mann-Whitney-U test, $p < 1.10^{-11}$).

Of a total of 122 eligible FS-pMSN pairs, we identified 63 cross-correlograms (51.6 %) exhibiting peaks or troughs that were significantly different from baseline in at least one

time window (see Eperimental Procedures). Of these 63 pairs, we will first describe the occurrence of troughs in pMSN firing when the FS unit was taken as reference cell, whereas other types of interaction will be discussed next. Based on the *in vitro* data on inhibitory FSI-to-MSN transmission (Koos and Tepper, 1999; Koos et al., 2004; Taverna et al., 2007), the straightforward prediction can be made that FS firing should be followed, at least in some cases, by a trough in pMSN firing at a relatively short latency. Troughs in pMSN firing associated with FS spiking were indeed encountered in 17 pairs, but with an average trough latency of -7.4 ± 3.5 ms (range: -30 to +30 ms; Fig. 3.2A,B). Surprisingly, only 2 out of 17 pairs exhibited a trough latency > 0 ms; when a trough was present, its onset was usually clearly positioned < 0 ms. If rebound excitation of pMSNs would occur following FS firing, a trough in the cross-correlogram should be succeeded by an increment in correlated firing. Although such increments were occasionally found, they did not reach statistical significance.

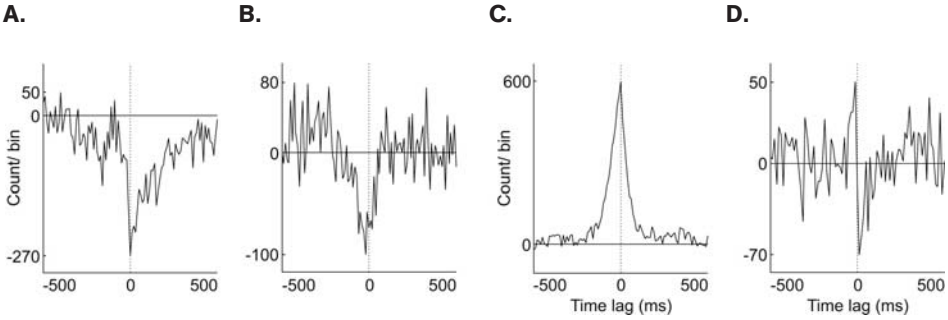

Figure 3.2

Cross-correlograms indicating temporal coordination between FS units and pMSNs in ventral striatum. All plots (A-D) represent cross-correlograms with an FS unit as reference cell and a pMSN as target cell. The time lag (x-axis) was divided in bins of 10 ms in (A-D) with zero time lag marked by a vertical line. On the ordinate the spike count per bin is plotted after subtraction of the spike count of the shuffled cross-correlogram. The expected mean level of spike counts is marked by the horizontal line, which is close to a spike count of zero due to shuffle-subtraction. Note the decrements in pMSN firing around the moment of FS unit firing (A, B), the steep, phasic increment (C) and the phasic increment followed by a decrement (D). All cross-correlograms (A-D) were recorded from different cell pairs.

Forty other pairs showed a monophasic peak of enhanced firing with latencies between -50 and +50 ms (mean ± sem: -11.3 ± 3.8 ms with FS unit as reference cell; Fig. 3.2C; some pairs with even longer latencies were found but not included here). A majority of these peaks were located at negative time lags, i.e. the FS predominantly fired after the

pMSN. Finally, six additional pairs displayed a peak followed by a though across more extended time lags (Fig.3.2D). The latency was -98.3 ± 38.8 ms and +60.0 ± 41.1 ms for peaks and troughs, respectively (range of peaks: -240 to -10 ms; troughs: 0 to +260 ms). No pairs were found exhibiting the temporally reverse combination, i.e., trough followed by peak.

Temporal relationships between firing patterns of units of the same type

Although most of the 20 FS units from the in *vivo* datasets were recorded in separate sessions, 11 FS-FS pairs were recorded simultaneously and on different tetrodes, and offered an opportunity to consider temporally coordinated firing amongst cells of this subpopulation. Seven significant interactions were observed (63.6 %). Four of the FS-FS pairs showed a rather broad, main peak sometimes accompanied by a narrower peak (-50 to 70 ms; N=2) on the shoulder of the main peak (Fig. 3.3A). The mean latency of the peak in the cross-correlogram was -12.5 ± 12.5 ms (range: -50 to 0 ms). Two other pairs showed a peak followed by a trough (Fig. 3.3B), with peaks ranging from: -200 to -100 ms and valleys from -50 to -10 ms. The remaining FS-FS pair with a significant interaction showed a singular trough with a latency of -25 ms.

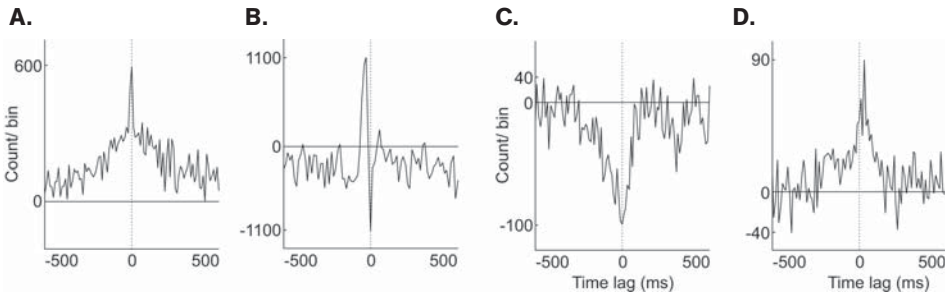

Figure 3.3

Cross-correlograms indicating temporal coordination between pairs of FS units (A,B) and pairs of pMSNs in ventral striatum (C,D). For explanation, see Fig 3.2. Pairs of FS units show episodes of enhanced concurrent firing over narrow as well as broader time ranges (A), or phasic increments followed by a decrement (B). Temporal firing relationships between pMSNs comprise decrements in pMSN firing around the time that another pMSN fires (C), or transient peaks of concurrent firing with time lags close to zero (D).

Finally, we considered pMSN-pMSN firing relationships, which may be predicted to be dominated by unidirectional, lateral inhibition mediated by $GABA_A$-receptors (Czubayko and Plenz, 2002; Tunstall et al., 2002; Koos et al., 2004; Taverna et al., 2004; Venance

et al., 2004). Of the eligible pairs a majority (13 out of 17, 76.5%) showed a significant temporal relationship. Six pairs showed a trough in firing, with a latency of -8.3 ± 8.3 ms (range: -50 to 0 ms; Fig. 3.3C). Seven other pairs showed a concurrent increment of firing, with peaks around or slightly in advance of 0 ms (-14.3 ± 9.2 ms; range: -50 to 0 ms; Fig. 3.3D). In pairs of this type, a combination of a peak and trough was not found.

Behavioral correlates of fast-spiking unit activity

We considered how firing-rate patterns of FS units were spatially distributed across the triangular track that was used for the reward-searching task. These FS units (N=10) were all recorded in Experiment 1 and thus form a subset of the 20 FS units used for computing cross-correlograms. By running unidirectionally along this track (Fig. 3.4), rats encountered rewards of 3 different types at 3 specified sites with an average probability of 33%, each reward type being associated with one of these 3 places.

The mean firing rate of the FS units during track running was 21.5 ± 4.0 Hz (N=10). In all but one of these units we found statistically significant deviations from baseline firing in close correlation with one or multiple task events. Although the specific response patterns were heterogeneous, one common feature was found in all of these behaviorally modulated FS units: their firing rate consistently decreased, often for several consecutive seconds, when the rat encountered and consumed a reward at one, two or all three sites (Fig. 3.4A, B). When the rat stopped at a reward site but did not receive a reward, no clear decrement was present except for one unit. Prior to arrival at a reward site, the FS units exhibited a variety of firing behaviors. Four out of 9 FS units exhibited a gradual increase in firing rate ("ramping") when the rat approached one or more reward sites (Fig. 3.4A, site 1) whereas 2 units showed a gradual decrease. Of the 3 remaining cells, 2 showed a brief peak in firing just before arrival at the reward site, whereas one unit did not show significant pre-reward activity. It is possible that the firing-rate changes generated directly (i.e. within ~20 cm) in advance of reaching the reward site contain a component of reward identification by e.g. smell or sight.

In comparison, pMSNs showed a much lower average firing rate (0.23 ± 0.05 Hz, N= 190, Table 3.1) during track running than the 10 FS units recorded in the same sessions ($p < 1.\ 10^{-6}$, Mann Whitney's U-test; these 190 pMSNs include the pMSNs from Experiment 1 used for the cross-correlation analysis, plus the simultaneously recorded units that lacked sufficient spike activity to be eligible for this analysis, but satisfied the ISVD-HDT criteria for classification in the pMSN group. Of these 190 units, 15 showed a significant behavioral correlate; this low percentage (7.9 %) is at least partly due to the large proportion of

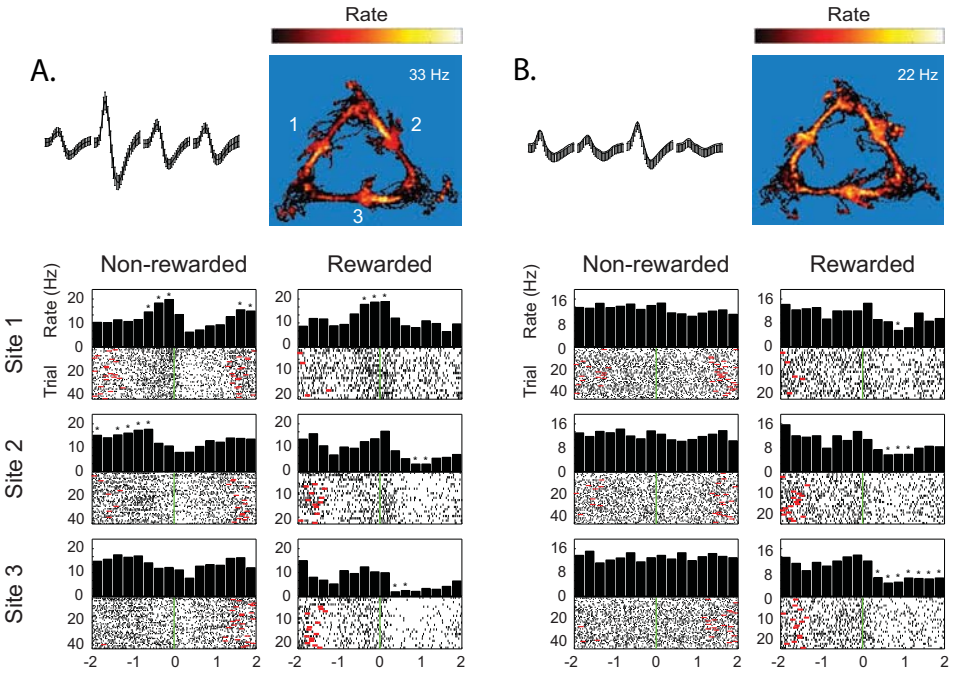
A.
Rate
33 Hz
1
2
3
B.
Rate
22 Hz
Non-rewarded
Rewarded
Site 1
Site 2
Site 3
Rate (Hz)
Trial
Time (s)

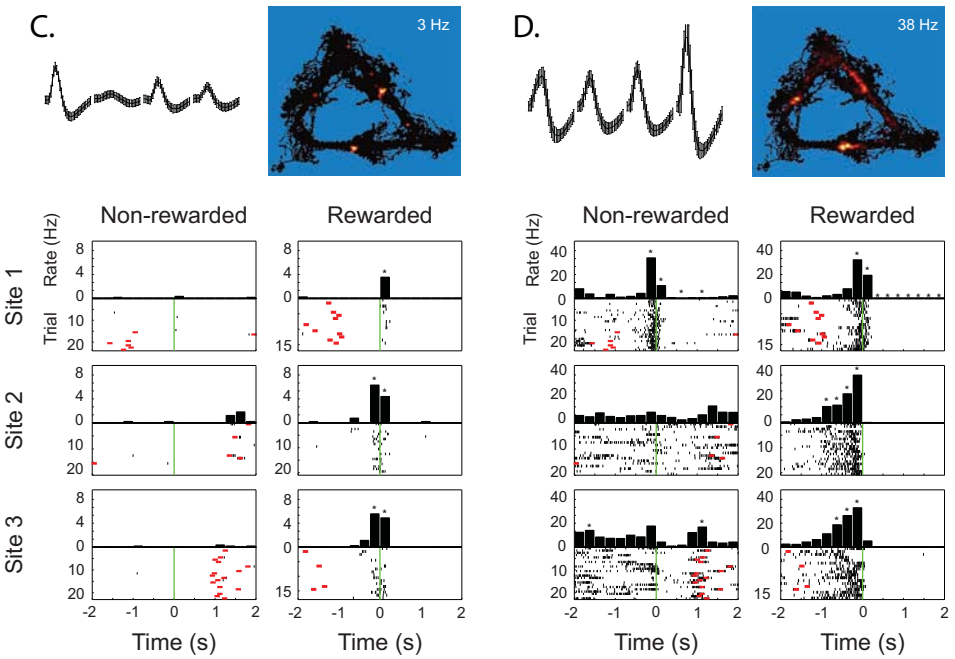
C.
3 Hz
D.
38 Hz
Non-rewarded
Rewarded
Site 1
Site 2
Site 3
Rate (Hz)
Trial
Time (s)

◀ Figure 3.4

Behavioral correlates of four ventral striatal neurons (A-D) as observed during reward searching behavior on a triangular track. The waveforms of the neurons recorded across the four leads of a tetrode are shown in the top left corner of each panel. The first two units were identified as FS units (A and B), while (C and D) show putative MSNs for comparison. The upper right side of each panel shows the spatial distribution of firing rate ('rate map'). The units were taken from different behavioral sessions; for all cases the running direction was clockwise. The color of each bin represents the local firing rate of each unit. Firing rates range from 0 Hz (black) to a maximum (white) that varies from unit to unit and is specified at the top right of each rate map. White numerals in (A) apply to all three rate maps and refer to the reward sites and the types of reward allocated to each site (1: sucrose; 2: vanilla dessert; 3: chocolate mousse). The bottom graphs in each panel show peri-event time histograms for the six types of behavioral events in the task (visits to all three reward sites, each one of which was coupled to a specific reward type; visits were specified according to the presence or absence of reward). The synchronizing time point (t=0 s) was the moment the rat crossed a line perpendicular to its running trajectory just prior to arriving at a reward site. Arrivals at other reward sites are indicated by grey ticks in the raster plots. Histogram bars represent average firing rate in bins of 250 ms; asterisks mark statistically significant deviations from baseline (Wilcoxon's matched-pairs signed-rank test, $p < 0.01$). Note the decrements in firing rate following two (A) or three (B) types of reward in the FS histograms. In contrast, the pMSNs show increments in firing rate, either a transient increase just prior and after arrival at each reward site (C) or a gradually increasing firing rate prior to reward site arrival (D). Additional decrements in FS rate are visible at multiple corners of the triangular track. The FS unit in (A) showed a significantly stronger decrease to the chocolate-mousse reward at site 3 as compared to sucrose at site 1 (Kruskal-Wallis test, $p < 0.05$, followed by Mann-Whitney's U-test, $p < 0.05$). Moreover, for all three reward sites the response pattern upon reward was significantly different from the non-rewarded condition (Mann-Whitney's U-test, $p < 0.05$). The responses to reward of the FS unit in (B) all differed significantly from each other, showing progressively more suppression of firing rate from sucrose to vanilla to chocolate. Significant differences between the rewarded and non-reward conditions were found for sites 1 (vanilla) and 3 (chocolate). The pMSNs (C and D) exhibited a significant difference between the reward conditions at site 2 and 3 versus 1 (vanilla, chocolate and sucrose, respectively). In addition, all three reward sites in (C) showed a significant difference for rewarded versus non-rewarded conditions whereas in (D) responses for sites 2 (vanilla) and 3 (chocolate) were different for reward presence versus absence.

units generating only few spikes during track running, making a robust assessment of the pattern's statistical significance in this subgroup difficult. The nature of these 15 correlates was heterogeneous and included both pre- and post-reward responses. When pMSNs showed a significant change in firing rate upon encountering and consuming a reward (10 units, 66.7 %), the change uniformly consisted of a firing rate increment (Fig.3.4 C,D). Thus,

their reward responsiveness was largely opposite in sign to that of FS units. Halting at a reward site where neurons. The remaining 3 units with correlates exhibited a general firing-rate increment upon arrival at a reward site, but these increments reached significance only when both reward and non-reward events were taken together. As was the case for FS units, pMSNs exhibited a variety of firing behaviors prior to arrival at a reward site, including ramp-like increments in firing rate (Fig. 3.4D) or brief pre-reward peaks (Fig.3.4C).

Discussion

Using multi-neuron recordings with tetrode arrays in freely behaving and resting rats, we studied the firing behavior of FS units and pMSNs of the ventral striatum in relation to behavioral events in a reward-searching task. These two cell types could be distinguished on the basis of their spike waveforms and their mean firing rates could be used as an additional criterion to differentiate them. When analyzing cross-correlograms between pairs of FS and pMSN units while the animal was at rest, a subset of pMSN units showed a pronounced trough in firing density when FS units spiked. However, this decrement in pMSN firing usually commenced already before the moment of FS spiking, which would contradict a simple scheme of a direct, monosynaptic inhibition. In addition, cross-correlograms of FS pairs often showed rather broad peaks of concurrent firing, although other interactions such as combinations of peaks and troughs were also encountered. Upon studying behavioral correlates of firing-rate changes of pMSNs and FS units during a reward-search task, FS units generally showed a decrease upon reward consumption, whereas a large majority of pMSNs increased their firing rate during this event.

Classification of fast-spiking and putative medium-sized spiny neurons

A foremost point for discussion is whether these extracellularly recorded classes of units can actually be identified as parvalbumin-positive fast-spiking interneurons and medium-sized spiny neurons. First, the much higher abundance of pMSNs than FS units agrees with the fact that MSNs make up ~90-95% of the total cell population in the striatum (Kemp and Powell, 1971; Groves, 1983; Chang and Kitai, 1985; Gerfen and Wilson, 1996), whereas parvalbumin-positive interneurons are estimated to comprise ~0.7% of striatal cells by stereological accounts (Luk and Sadikot, 2001). That the relative percentage of FS units in our sample is higher than immunocytochemically estimated can be explained by the low mean firing rate of MSNs *in vivo* and their low excitability *in vitro* (Wilson and Groves, 1981; Uchimura et al., 1989; Pennartz et al., 1991; 1994; Wilson, 1993; Stern et al., 1998; Taverna et al., 2004; Mahon et al., 2006) and the consequent difficulty to identify clusters with very low spike counts as belonging to a distinct unit. Second, the spike properties of ventral striatal FS units resemble those of immunocytochemically identified

FS interneurons *in vitro* (Taverna et al., 2007; cf. Kawaguchi, 1993; Kawaguchi et al., 1995), especially in their short spike duration, rapid and strong spike afterhyperpolarization and ability to fire at high frequencies. When the second derivative of action potentials of identified FS interneurons, recorded in whole-cell mode *in vitro*, was computed, clusters of decay parameters were found to overlap with the clusters recorded *in vivo* and to be distinct from clusters of identified MSNs (Taverna and Pennartz, unpublished data; cf. Taverna et al., 2007). In contrast, both pMSNs (Fig. 3.1) and MSNs, identified *in vivo* and *in vitro* respectively, show broader action potentials and slower decay and spike afterhyperpolarization and reach only low mean firing rates (cf. Berke et al., 2004). That these neurons were mostly transiently active while the rat performed the reward-searching task fits their profile as phasically active neurons (Wilson and Groves, 1981; Kimura et al., 1996; Shibata et al., 2001; Mahon et al., 2006). The current study adds a new element to the palette of criteria for distinguishing different types of striatal neurons *in vivo*, viz. the opposite response pattern of FS and pMSNs units to reward consumption, as further discussed below. Despite the availability of various distinguishing criteria, however, it should be emphasized that the immunocytochemical identity of a given type cannot be proven by extracellular recordings, and caution should be exerted in interpreting recorded spike patterns as belonging to a certain type. In particular, FS and pMSN samples might have contained small subgroups of less well-characterized striatal interneurons.

Temporal relationships between firing patterns

The temporal relationships between firing patterns of putative FS units and pMSNs were studied by computing cross-correlograms from spike trains recorded while the animals were resting or sleeping. This part of the study primarily yielded insights into FS-pMSN interactions (122 pairs), while smaller samples of FS-FS and pMSN-pMSN pairs were assessed in addition. Of the FS-pMSN pairs showing a significant deviation from baseline in the cross-correlogram, a substantial number (17 out of 63, 27.0%) showed a trough in pMSN firing around the moment of FS spiking. However, in contrast to the prediction that MSN firing is inhibited via a direct, monosynaptic input from FS interneurons, which would be expressed as a trough in the cross-correlogram with a time lag $>$ 0 ms, the average trough latency was actually negative to zero (Fig. 3.2A,B).

Considering the evidence for the powerful and widespread nature of FS-to-MSN inhibition in striatum (Koos and Tepper, 1999; Taverna et al., 2007), this finding may seem surprising at first, but can be explained when the patterns in FS-FS cross-correlograms are also taken into account. The dominant pattern found in these relationships was a rather broad peak of concurrent firing (Fig 3.3A; 4 out of 7 pairs, 57.1%), sometimes accompanied

by a trough (Fig.3.3B). Apparently, when a FS unit fires there is a high probability of another FS unit spiking already beforehand, which can be explained from a configuration in which at least some FS units receive excitatory input and engage in mutual excitatory interactions via gap junction coupling. Indeed there is evidence for electrotonic coupling amongst FS interneurons (Koos and Tepper, 1999; Taverna and Pennartz, 2008) as well as for glutamatergic inputs onto FS interneurons from neocortical, amygdaloid, hippocampal and/or thalamic structures (Kita et al., 1990; Pennartz and Kitai, 1991; Bennett and Bolam, 1994; Plenz and Kitai, 1998). When current anatomical and electrophysiological knowledge is combined with the present observation of troughs in pMSN activity already commencing before FS firing, the scheme emerging is that of a 'reticular' system of electrotonically coupled FS interneurons that can be rather easily excited by limbic-cortical input to one locus of the system and that subsequently inhibit MSNs situated at other loci of the same system. Thus, we propose that the collective results can be most parsimoniously explained by an interconnected network of FS interneurons providing a fast, 'early' inhibition onto striatal projection neurons, once this network receives either a global or restricted excitatory input. This configuration is well compatible with earlier proposals for FS interneurons mediating feed-forward inhibition, but extends this idea in a major way by suggesting that feed-forward inhibition is mediated by a broadly synchronized network of interneurons (Fig. 3.5).

Nonetheless, it should be kept in mind that alternative explanations for the troughs in pMSN activity around the moment of FS firing cannot be excluded. Lateral (or recurrent) inhibition between MSNs might play a role, although experimental evidence indicates that individual MSN-MSN synapses may be too weak to significantly affect firing and that FSI-MSN synapses are more effective in doing so (Tunstall et al., 2002; Koos et al., 2004; Taverna et al., 2004; 2007). Also, an external inhibitory input to MSNs that is somehow coordinated with FS unit firing would be compatible with the results, but the only likely source of extrinsic GABAergic inputs to the VS is the ventral pallidum (Hakan et al., 1992; Groenewegen et al., 1993) and these inputs are known to synapse primarily onto parvalbumin-positive interneurons, not MSNs (Kita, 1993; Bevan et al., 1998; Bolam et al., 2000). Apart from the predominant patterns in FS-pMSN and FS-FS cross-correlograms discussed above, other types of temporal coordination were observed. For FS-pMSN pairs, these types of interaction comprised peaks of concurrent firing (Fig. 3.2C) or a combination of a peak followed by a trough (Fig. 3.2D). These peaks can be most parsimoniously explained by the FS unit and pMSN receiving temporally coherent, glutamatergic inputs from afferent areas, although other explanations cannot be excluded. That some of the troughs in pMSN firing were preceded by a peak is well compatible with a feed-forward

inhibitory circuit in which limbic-cortical input may excite the MSN already before FSI firing and before the onset of inhibition by the interneuron (cf. Pennartz and Kitai, 1991), as well as with the network scheme proposed above. Clear indications for a rebound excitation following a trough in pMSN firing density were not found.

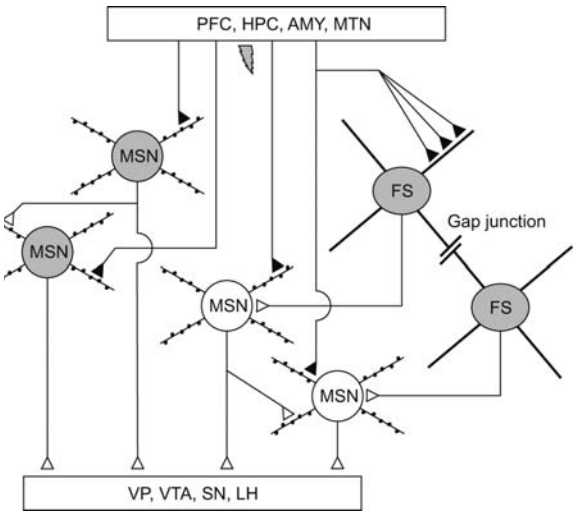

Figure 3.5
Schematic representation of the interactions between fast-spiking interneurons and medium-sized spiny neurons, proposed to underlie the observed cross-correlation patterns. FSIs and MSNs both receive excitatory glutamatergic input from cortico-limbic structures (glutamatergic synapses are indicated with black triangles, excited neurons are colored grey). Through electrotonic coupling of FSIs, restricted cortico-limbic input may lead to the activation of a network of FSIs, thereby providing a widespread, broadly synchronized inhibition on the MSN population (inhibited units and GABAergic synapses are depicted in white and open triangles respectively). Thus, also MSNs that are not synaptically connected to FSIs receiving monosynaptic glutamatergic input can be inhibited upon activation of the FSI network. Axonal branches of MSNs make functional, unidirectional GABAergic synaptic contacts onto dendrites of nearby MSNs. Such single-cell mediated inhibition, however, is likely too weak to directly influence the firing of the postsynaptic MSN. PFC: prefrontal cortex; HPC: hippocampus; AMY: amygdala; MTN: midline thalamic nuclei; VP: ventral pallidum; VTA: ventral tegmental area; SN: substantia nigra; LH: lateral hypothalamus.

Besides FS-pMSN and FS-FS cross-correlograms we also studied firing relationships between pairs of pMSNs. This analysis produced evidence for broadly concurrent firing in about half of the eligible pairs (Fig.3.3D), which may be explained by a common, but temporally dispersed glutamatergic input. In the other eligible pMSN-pMSN pairs, comprising almost 50% of this group, troughs in firing density of pMSN target cells were found around the moment the other member of the paired fired (Fig. 3.3C). Because these troughs spanned both positive and negative time lags (as in the case of FS-pMSN interactions, e.g. Fig. 3.2B), they cannot be directly explained by a scheme of direct lateral (or recurrent) inhibition between individual pMSNs. Two possible explanations hold that

(i) the trough commences early because other pMSNs are crudely synchronized with the reference pMSN under scrutiny (Fig. 3.3D) and already inhibit the target pMSN by way of their axon collaterals before the reference cell fires, or (ii) FS interneurons provide an ´early´ inhibition of the target MSN but do not suppress firing in the reference MSN. Which of these schemes applies is a question awaiting further investigation.

Behavioral correlates of fast spiking unit activity

In studying the behavioral correlates of *in vivo* FS firing patterns, a striking general feature was noted, viz. the suppression of firing rate during and following reward consumption. In contrast, pMSNs recorded in the same sessions showed a predominant firing-rate increase in the same task phase, while pre-reward changes in firing behavior were rather heterogeneous for both cell groups. First, these results suggest a fine-grained coding or information-processing capacity for FSIs in the VS. Our finding that FS units did not show a firing decrement when the animal halted but received no reward suggests that a cessation of locomotor activity cannot explain the observed correlate. However, it will require further studies to elucidate the exact task-related parameters encoded by FSI firing rate as they may include sensory, motor and motivational aspects of reward consumption.

Second, the contrast between post-reward decrements in FS activity versus predominant increments in pMSN activity (Fig. 3.4) suggests a functionally dissociable and opposing role of these cell types during reinforcement processing in general. These findings lead to the hypothesis that a reward-related decrement of FSI firing may be coupled to a partial release of MSNs from inhibition, resulting in an enhanced VS output signal propagated to target structures such as the ventral tegmental area and ventral pallidum, as well as a widening of the temporal window for the induction of long-lasting changes in glutamatergic synaptic contacts onto MSNs, which is under GABAergic control (Pennartz et al., 1993). Such long-term plasticity has been postulated to subserve the storage and consolidation of associative coupling of sensory cues and motor actions to reinforcement contingencies (Robbins and Everitt, 1996; Kelley et al., 1997; Pennartz et al., 2002; Dalley et al., 2005).

Further implications and conclusions

While the distinct reward-related decrements in FS unit firing during the reward-search task on the triangular track are consistent with their role in coding task-related information, it is equally important to consider their potential functions in mediating rhythmic mass activity in the dorsal and ventral striatum. Various forms of rhythmic EEG activity have been

described in VS, although it has not been always ascertained whether these rhythms truly originate from the VS itself. In an awake, immobile state and during face washing, delta-like (0.5 – 3 Hz) rhythms have been described in the VS of freely moving rats (Leung and Yim, 1993), whereas during behavioral performance in a radial-maze task, theta (~8 Hz), beta (~20 Hz) and gamma (~50 Hz) activity has been reported (Berke et al., 2004; cf. Masimore et al., 2005). By virtue of the strong monosynaptic connectivity between bursting FSIs and MSNs (Koos and Tepper, 1999; Taverna et al., 2007), it has been suggested that FS interneuron firing may help to entrain MSN activity to particular rhythms (cf. Berke et al., 2004) and it is noteworthy that the burst frequency of FS interneurons *in vitro* (~2.4 Hz) falls within the delta-frequency range, whereas their intra-burst firing rate (~52 Hz) lies within the gamma range (Taverna et al., 2007). The current evidence gathered from active behavioral and resting phases is well compatible with a role for FS interneurons in coordinating or entraining striatal principal cell activity because, first, their firing-rate changes were generally of opposite sign with respect to the firing increments of pMSNs during reward consumption; such opposing excitability changes in FS and pMSN subpopulations may be well reflected in periodic mass phenomena, although this issue deserves further investigation. Second, the various configurations of troughs, peaks or combinations thereof in the cross-correlograms indicate widespread, diverse forms of temporal coordination amongst FS and pMSN subpopulations which may well be expressed in transient oscillatory activity at the more macroscopic level of field potentials. To what extent subgroups of FS interneurons and MSN synchronize and phase-lock to oscillations in various frequency bands remains to be investigated, although a tight temporal relationship between FS firing and theta rhythm has been previously reported for the VS (Berke et al., 2004). It will be equally worthwhile to examine how the various forms of temporal coordination (Fig. 3.2 and 3.3) depend on the state of corticostriatal networks, for instance during different sleep phases (slow-wave or REM sleep) or during bouts of theta or gamma activity appearing during active behavior.

In conclusion, the current data indicate that firing patterns of VS FS units - contrary to those of pMSNs - display distinct post-reward decrements in firing rate, which supports a function for FS interneurons in fast information processing during reward-consumption and related behavior. Furthermore, cross-correlograms for firing patterns of FS and pMSN units revealed a variety of temporal relationships, of which the most significant were patterns of concurrent FS-FS firing and decrements in pMSN firing density around the time a FS unit spiked. These results are consistent with a rather broadly synchronized network of interneurons that selectively suppresses firing activity of striatal projection neurons.

Experimental Procedure

Behavioral procedures and unit recordings.

Ten sessions of unit recordings from non-anesthetized animals were obtained from 4 rats, comprising ensembles of 14-19 simultaneously recorded ventral striatal units per session. Spike datasets were taken from two experiments designated as Experiment 1 and 2. From Experiment 1 (2 rats, 6 sessions) we used spike data from a post-behavioral rest/sleep phase as well as from the task that preceded it, involving food search and running along a triangular track. From Experiment 2 (2 rats, 4 sessions) we only used spike data from a rest/sleep phase occurring after the rats had been performing a T-maze task. All procedures were performed following the Netherlands and National Institutes of Health (U.S.A.) guidelines for the use of vertebrate animals in research.

Behavioral procedures in Experiment 1. Subjects were adult male Wistar rats (375-425 g, Harlan, the Netherlands). Animals were housed individually, weighed and handled daily and kept on a 12:12 light/dark cycle with lights on at 8:00 AM throughout the training and recording period. Animals had access to water in the home cage for a 2-hour period following each training session but had *ad libitum* access to food. Following pre-training on a linear track, surgery and recovery, rats were introduced to a task in which they were required to search for reinforcement by running in one direction along a triangular track (length of equilateral sides, 90 cm, width 10 cm). The types of reinforcement were 10% sucrose solution, vanilla desert or chocolate mousse, with each of these reward types applied to a corresponding cup, placed at the center of one of the triangle sides. Thus, each type of reward was assigned to a fixed cup location throughout all recording sessions of a single rat. A single reward was delivered to one of the three cups during a full lap along the triangle according to a pseudorandom schedule. The triangle task, lasting about 20 min., was flanked by two rest/sleep periods (rest 1, 20-60 min.; rest 2, 60-120 min.) during which the rat stayed in a “nest”, i.e. a towel folded into a deep plate on a flower pot located next to the track. Because the second, post-behavioral resting period presented the longest recording episode of the session devoid of controlled behavioral events which may affect firing relationships such as synchrony, cross-correlations were computed from this period.

Behavioral procedures in Experiment 2. Subjects were adult male Fisher 344 rats (Charles River Laboratories, Wilmington, MA) weighing 320-340 g. Housing conditions were similar to Experiment 1, except that lights went on at 10:00 PM. Water and food (rat chow, 4% mouse/rat diet 7001, Harlan Teklad, Madison WI, U.S.A.) were available *ad libitum* until 8-4 days before surgery. During the training and recording periods, rats were maintained at 80% of their weights as observed under ad libitum conditions and had access to water at all times.

A complete recording session consisted of a pre-task rest/sleep period lasting 15-30 minutes, a T-maze task lasting 10-20 minutes in which food-deprived rats learned to forage for food rewards that were distributed at the arm ends according to a probabilistic schedule, followed by a post-task resting period lasting 15-40 minutes (Pennartz et al., 2004). Spike data from the postbehavioral rest period of Experiment 2 were used to compute cross-correlations but not to analyze behavioral correlates of unit activity. The rationale for this restricted use of Experiment 2 was that the structure of the triangular task of Experiment 1 incorporated a unidirectionality of track exploration, which was more suitable for analysis of behavioral correlates of interneuron firing patterns than in the case of Experiment 2. Since the electrophysiological and analysis methods for the two experiments were very similar, we will only indicate the main differences in the section below.

Surgery and Electrophysiology. Tetrodes (diameter ~30 μm) were used to obtain stable, parallel recordings from many well-isolated single units (McNaughton et al., 1983a; Recce and O'Keefe, 1989; Gray et al., 1995). In Experiment 1, we used a "split drive" targeting one bundle with 7 tetrodes to the VS and a second bundle with additional tetrodes to hippocampal area CA1 while 2 reference electrodes were placed in the corpus callosum and hippocampal fissure. In Experiment 2, a multi-electrode drive containing 12 tetrodes was implanted unilaterally above the VS of each rat, while four electrodes were placed in the neocortex and hippocampus to serve as a reference and to record neo- and archicortical EEG traces. Hippocampal recordings were not addressed in this paper.

For implantation, animals were anaesthetized in Experiment 1 with 0.08 ml/100 g body weight Hypnorm i.m. (0.2 mg/ml fentanyl and 10 mg/ml fluanison; Janssen Pharmaceutics, Beerse, Belgium) and 0.04 ml/100 g Dormicum s.c. (midazolam 1.0 mg/kg; Roche Netherlands, Woerden); in Experiment 2 we used sodium pentobarbital (40 mg Nembutal / kg body weight i.p.). Rats were mounted in a Kopf stereotaxic frame. The exit port of the tetrode bundle targeting the VS was centered on 1.7 mm anterior and 1.3 mm lateral to bregma (Paxinos and Watson, 1986). Recording sessions were initiated as soon as all tetrodes were estimated to have entered the VS. On consecutive recording days, individual tetrodes were usually lowered further. Spikes were captured by taking a 1 msec data sample at 32 kHz whenever the voltage signal exceeded a preset voltage threshold, using a Cheetah ADC interface (Neuralynx, Bozeman, MT, U.S.A.; amplifier gain: 5000X, band-pass filtering: 0.6 – 6.0 kHz). The headstage contained an array of light-emitting diodes which allowed video-tracking of the rat's head position, using a camera situated about 1.5 m above the behavioral setup. The spatial and temporal resolution of the videotracking system were 2.5 mm/pixel and 16.7 ms (i.e., 1/60 Hz^{-1}), respectively. In addition, the behavior of all rats was recorded on analogue videotape.

Data analysis

Single units were discriminated off-line using established cluster-cutting methodology (BubbleClust and MClust; cf. Mizumori et al., 1989; Gray et al., 1995). Spike interval histograms, autocorrelograms and average spike waveforms were checked before a putative cluster of spikes was accepted as belonging to one unit. To seek spike parameters optimally suited to distinguish fast-spiking (FS) units from putative medium-sized spiny neurons (pMSNs), we initially quantified a number of waveform parameters, including the initial rising slope, spike half-width, ratio of peak and valley amplitude, valley half-decay time (HDT), initial slope of valley decay (ISVD) and delay from valley minimum until return to baseline. The ISVD was calculated as follows:

$$ISVD = -100 .(V_v-V_{0.26})/A_{pv} \quad (EQ.1)$$

where V_v is the most negative value (valley point) of the spike waveform, $V_{0.26}$ the voltage at 0.26 ms after V_v, and A_{pv} the peak-to-valley amplitude (Fig. 3.1A). The HDT was defined as the time interval during which the valley decayed back to its half-maximal value (Fig. 3.1B).

Although many previous studies have traditionally focused on spike width as a criterion to distinguish FS interneurons (e.g. Constantinidis and Goldman-Rakic, 2002; Berke et al., 2004), criteria derived from the rate of valley decay yielded a clearer group separation for the data presented here than the former measure. Moreover, all spike waveform measures were also applied to the second derivatives of averaged action potentials recorded from immunocytochemically identified fast-spiking interneurons and medium-sized spiny neurons in a previous whole-cell patch-clamp study (Taverna et al., 2007; cf. Lorente de No', 1947; Phillips, 1973), and also here the two types of identified neurons could be best separated using the valley decay parameters HDT and ISVD. However, it should be emphasized that extracellular recording methods, regardless of the precise classification method chosen, do not provide a strict verification of the phenotype of recorded neurons.

Using a fuzzy-clustering algorithm (see: Fuzzy Clustering and Data Analysis Toolbox, http://www.fmt.vein.hu/softcomp/fclusttoolbox; cf. Bezdek, 1981) on the ISVD and HDT data of 148 ventral striatal units elegible for cross-correlogram analysis, two groups of neurons were delineated. This type of clustering algorithm has the advantage that it provides an indication about the certainty that a given data point belongs to a certain cluster, thus making its in- or exclusion less arbitrary than is usually the case. In fuzzy clustering, the algorithm provides a value, bounded between 0 and 1, representing the certainty that a

neuron belonged to either group. Neurons that were not classified into one single group, based on a certainty-measure larger than 0.8, were removed from the dataset (14 out of 148). The final dataset contained 134 ventral striatal units, of which 114 were classified as pMSN and 20 as FS unit.

To illustrate the degree to which pMSNs and FS units were separated using the clustering algorithm, their average ISVD values were 15.0 ± 0.3 (N=114) and 35.0 ± 1.1 (N=20), respectively. HDT values for MSNs and FSIs were 0.31 ± 0.00 ms and 0.20 ± 0.00 ms.

Cross-correlograms, based on the spike datasets from the postbehavioral rest/sleep phases in Experiment 1 and 2, were constructed according to Perkel et al. (1967) and Eggermont (1992). Cross-correlation data from both experiments were similar and therefore pooled. A spike shuffling-subtraction procedure was applied (Perkel et al., 1967; Aertsen et al., 1989). Because exact significance levels are notoriously difficult to derive from these histograms, we adopted Eggermont's procedure (1992) to compute the mean expected number of joint spike counts, μ, and the levels of $\mu \pm 3$*SD (SD, standard deviation; corresponding to p=0.0013) to provide at least crude indications for non-random excursions of spike counts above or below the expected range. These indicators are considered crude because the expected mean and SD of spike count are estimated under the assumptions of Poisson-distributed spike trains and of independence of the two spike trains. Cross-correlograms were only analyzed when cell pairs were recorded on different tetrodes and produced sufficient spike counts across the sampling period; the threshold for eligibility was a joint product of mean firing rates of 2.0 Hz^2.

Cross-correlograms were primarily assessed using a bin size of 10 ms (range of time window: -500 to +500 ms). To study temporal relationships at both coarser and more fine-grained resolutions, we used bin sizes of 1 and 50 ms in addition (windows: [-50, +50] and [-2000, +2000] ms, respectively). Peaks and troughs with a latency of ± 50 ms with respect to time lag zero were taken into account. Finally, we subjected each cross-correlogram to five different shuffle subtractions and only accepted peaks or troughs when trespassing the 3*SD boundary above or below the mean on each of these 5 occasions. The overall procedure is rather conservative, first because of the fact that the 3*SD boundaries were based on non-subtracted cross-correlograms and noise is added by shuffle subtraction, and second because of the five-fold repetition of shuffle subtractions.

Behavioral correlates of firing patterns of single units were evaluated using rate maps and peri-event time histograms using the spike datasets from Experiment 1 (Fig. 3.4). Rate

maps, i.e. graphs displaying a single unit's firing rate as a function of the spatial position of the rat's head on the triangular track, were constructed by dividing the track in spatial bins 0.75 cm in width, counting the rat's occupancy time and number of spikes allocated to each bin based on the time stamps of spikes and head positions, and dividing the spike count by the occupancy time. Bins with very low occupancy (< 0.167 s across the total behavioral period) were not assigned a primary firing rate value. A secondary, final firing rate value for each bin was obtained by a spatial smoothing procedure in which each bin's primary firing rate value was averaged with the primary values from its four nearest neighboring bins. Peri-event time histograms were constructed by installing, off-line, three "virtual photobeams" on the triangular track, each of which was positioned so as to signal the rat's arrival at a reward site. The moment of crossing this line was taken as the synchronizing time point for the histograms. Using videotape information, peri-event time histograms were constructed for the two different conditions (rewarded/non-rewarded) per site, thus yielding 6 different histograms. To determine whether a unit exhibited a significant change in firing rate in relation to each of the 3 reward sites, we considered time bins of 250 ms within a period of 1 s before to 1 s after a reward site crossing, which did not reflect responses in relation to previously or subsequently visited reward sites. Using Wilcoxon's matched-pairs signed-rank test ($p < 0.01$), we assessed whether the spike count for each bin close to a reward-site crossing ('test bin') was significantly different from the spike count within the same trial in each of three reference bins, which were located in the corner section of the track opposite to the reward site under study. We controlled for the possibility that a marked change in firing rate occurred in that corner, which was not the case for the units presented here. A firing rate change was only considered significant if the spike count in the test bin met the $p < 0.01$ criterion for all three reference bins. Differences between responses at the three reward sites were statistically evaluated with a Kruskal-Wallis test ($p < 0.05$) followed by Mann-Whitney's U-test ($p < 0.05$), while rewarded versus non-rewarded conditions were compared using Mann-Whitney's U-test ($p < 0.05$).

Histology

At the end of an experiment the positions of tetrodes were marked by passing a 10 s, 25 μA current through one lead of each tetrode. Rats were transcardially perfused with 0.9 % saline solution followed by 4.0% paraformaldehyde in *experiment 1* and 4.0% paraformaldehyde and 0.05% glutaraldehyde in 0.1 M phosphate buffer (pH 7.4) in *experiment 2*. Brain sections were cut (40 μm) using a freezing microtome and Nissl stained to reconstruct tetrode tracks and their final positions as indicated by lesion sites. Localization of single units in the VS was verified using these histological reconstructions.

Acknowledgements

We wish to thank Bruce L. McNaughton and Carol A. Barnes (Tucson, Arizona) for the use of ensemble recording data gathered by CMAP in their laboratory (Experiment 2). We appreciate the efforts Jolanda Verheul made in the starting phase of analysis and her help with cluster cutting the data. The work of A. David Redish and P. Lipa in making the cluster-cutting programs MClust and BubbleClust available for use is gratefully acknowledged. This work was supported by the Netherlands Organization for Scientific Research VICI grant 918.46.609, HFSPO grant RGP-0127 and Grant BSIK-03053 from SenterNovem, the Netherlands.